Received: 18 January 2019 | Revised: 15 April 2019 | Accepted: 16 April 2019

DOI: 10.1002/jbm.a.36701

ORIGINAL ARTICLE

Dendrimer mediated targeting of siRNA against polo-like kinase for the treatment of triple negative breast cancer

Anjali Jain[1] | Shaheen Mahira[1] | Jean-Pierre Majoral[2] | Maria Bryszewska[3] | Wahid Khan[1] | Maksim Ionov[3]

[1]Department of Pharmaceutics, National Institute of Pharmaceutical Education & Research (NIPER), Hyderabad, India

[2]Laboratoire de Chimie de Coordination du CNRS (LCC), Toulouse, France

[3]Department of General Biophysics, Faculty of Biology and Environmental Protection, University of Lodz, Lodz, Poland

Correspondence
Wahid Khan, Department of Pharmaceutics, National Institute of Pharmaceutical Education and Research (NIPER), Hyderabad 500037, India.
Emails: wahid@niperhyd.ac.in, mail4wahid@gmail.com

Maksim Ionov, Department of General Biophysics, Faculty of Biology and Environmental Protection, University of Lodz, Lodz 90-301, Poland.
Email: maksim.ionov@biol.uni.lodz.pl

Funding information
India-Polish Inter-Governmental, Science & Technology Cooperation Programme, Grant/Award Number: DST/INT/POL/P-12/2014

Abstract

Irresponsiveness of triple negative breast cancer (TNBC) toward conventional therapies has drawn attention toward siRNA therapeutics. In gene delivery, dendrimers are gaining significant attention due to their characteristic features and polo-like kinase (PLK1) is reported as a potential target for TNBC. In this work, phosphorus and polyamidoamine dendrimer (generation 3 and 4 of each type) are explored to address delivery challenges of PLK1 siRNA (siPLK1). Dendriplexes were formed and complexation was found at 3:1 N/P ratio for all dendrimers by gel electrophoresis. Complexation was also supported by zeta potential, circular dichroism and intercalation assay. Dendriplexes were found to be stable in presence of ribonuclease and serum. Dendriplexes resulted in enhanced cell uptake of siPLK1 compared to siPLK1 solution in MDA-MB-231 and MCF-7 cells. Dendriplexes caused increased cell arrest in sub-G1 phase compared to solution. These observations suggested phosphorus and polyamidoamine dendrimers as potential carriers for siPLK1 delivery to treat TNBC.

KEYWORDS

dendriplex, phosphorus dendrimer, polo-like kinase 1, polyamidoamine dendrimer, small interfering RNA, triple negative breast cancer

1 | INTRODUCTION

Breast cancer is one of the leading causes of cancer death for women which is expressed in distinct forms with prognostic and therapeutic implications. Based upon the expression of estrogen receptor (ER), progesterone receptor (PR), and amplification of human epidermal growth factor receptor 2 (HER-2/Neu), breast cancer is categorized into subclasses such as hormone receptor positive tumors and HER-2/Neu amplified tumors (Brenton, Carey, Ahmed, & Caldas, 2005). The tumors which do not express ER, PR, and HER-2/Neu amplification are termed as triple negative breast cancer (TNBC) (Chavez, Garimella, & Lipkowitz, 2010). TNBC is considered as the most aggressive breast cancer (Dent et al., 2007). The complications in prognosis and treatment of TNBC exist due to lack of receptors on tumor surface, therefore the hormonal therapy and monoclonal antibodies are inapplicable to these patients (de Ruijter, Veeck, de Hoon, van Engeland, & Tjan-Heijnen, 2011).

Polo-like kinase 1 (PLK1) is reported as a potential therapeutic target for the treatment of TNBC (Hu, Law, Fotovati, & Dunn, 2012). PLK1, a highly conserved serine–threonine kinase is reported to be overexpressed in diverse cancer types and its expression is correlated with poor prognosis and aggressive behavior. Inhibition of PLK1 leads to mitotic arrest, interruption of cytokinesis and apoptosis in susceptible tumor cell populations (Strebhardt & Ullrich, 2006). However, delivery of siRNA to target site presents significant challenges due to its surface charge, hydrophilic nature, and high molecular weight (Pandi, Jain, Raju, & Khan, 2017). They are also susceptible to enzymatic degradation in plasma resulting in inadequate uptake at target site (Pecot, Calin, Coleman, Lopez-Berestein, & Sood, 2010).

To protect the siRNA from degradation and its delivery to target site, several nonviral carriers are explored (Jain, Hosseinkhani, Domb, & Khan, 2015; Pandi et al., 2017) and among them dendrimers gained significant attention due to their highly symmetric, hyperbranched spherical structure with defined surface charge. They display monodispersity, uniformity, definite surface charge (associated with the presence of numerous functionalizable terminal groups), and possibility for surface modification by ligand attachment.

In our previous work, three different class of dendrimers namely, polyamidoamine dendrimers (PAMAM), cationic phosphorus dendrimers (CPD), and carbosilane dendrimers (CBD) were explored as an alternative nonviral delivery system for delivery of cocktail siRNA from B-cell lymphoma (BCL) family. The cocktail mixture contained siBcl-xl, siBcl-2, siMcl-1 siRNAs, known to suppress the synthesis of anti-apoptotic proteins. The in vitro cell line studies using HeLa and HL-60 cells suggested the CPD as most effective among the three classes of dendrimer for the delivery of cocktail siRNA (Dzmitruk et al., 2015; Ionov et al., 2015). The outcomes unlocked the possibility for delivery of combination of siRNA through different classes of dendrimers in cancer cells.

This work is designed to explore the dendrimer mediated delivery of siPLK1 as an alternative treatment strategy for TNBC. For this purpose, PAMAM and CPD dendrimers of generation 3 and 4 are selected as per recommendation of our previous work (Ionov et al., 2012; Ionov et al., 2015; Pandi et al., 2018). The complexation and stability of dendriplexes is determined using different techniques. Cell uptake and cell cycle analysis of dendriplexes is performed in breast cancer cell lines (MDA-MB-231 and MCF-7). As MDA-MB-231 cell line is considered as model for expression of TNBC, the activity of dendriplexes against these cells would provide evidence toward the treatment of TNBC.

2 | METHODS

2.1 | Materials

Polo-like kinase 1 specific siRNA (siPLK1), sequence 5′UGAAGAAGA UCACCCUCCUU-AdTdT3′, Antisense 3′dTdTACUUCUUCUAGUGGG AGGAAU5′ and fluorescein isothiocyanate (FITC) labeled siPLK1 were purchased from Dharmacon™. Phosphorus dendrimer generation 3 and 4 (CPD 3 and CPD 4) 32 and 64 surface cationic end groups, respectively, were obtained as gift sample from Laboratoire de Chimie de Coordination du CNRS. PAMAM dendrimer generation 3 (PAMAM 3), PAMAM dendrimer generation 4 (PAMAM 4) 48 and 96 surface cationic end groups, respectively, triton X-100, diethyl pyro carbonate water, ethidium bromide and phosphate buffer saline (PBS) pH 7.4 were purchased from Sigma-Aldrich. The commercial PAMAM dendrimers are diluted in methanol, which can form strong bonds with both the hydrophobic and hydrophilic part of the dendrimer (Mdzinarashvili, Khvedelidze, Shekiladze, Shengelia, & Hianik, 2018). Prior experiments with siRNA due to remove the effects that can be caused by presence of organic solvent, the methanol has been evaporated from the dendrimer and after evaporation the dendrimer was diluted in water in appropriate concentration. Tris-EDTA buffer (TE; ×10 and ×1), ribonuclease (RNase) free water, agarose gel and bromophenol blue dye were purchased from Cleaver Scientific Pvt. Ltd., UK. Heparin was purchased from Gland Pharma Ltd., India. Quanti-iT™ Ribogreen® reagent and RNA standard stock were purchased from Life Technologies. Dulbecco's modified Eagle's medium (DMEM)-high glucose, fetal bovine serum (FBS), L-glutamine, antibiotic solution, antimycotic solution and PBS pH 7.2 were purchased from Life Technologies, Inc..

2.2 | Preparation of dendriplexes

Dendriplexes were prepared using our previously reported method with slight modification (Ionov et al., 2015; Pandi et al., 2018). siPLK1, dendrimer solutions, and sodium phosphate buffer (10 mM/L, pH 7.4) were mixed at predetermined concentrations to obtain desired N/P molar ratio. The mixture was incubated for 10 min at 22°C.

2.3 | Gel retardation and integrity assay

Agarose gel electrophoresis was used to study the formation of siPLK1 dendriplexes and to determine the dendrimer mediated protection of siPLK1 from ribonucleolytic degradation (Du et al., 2012). Dendriplexes of siPLK1 with CPD 3, CPD 4, PAMAM 3, and PAMAM 4 were prepared from N/P ratio 0.5:1 to 10:1. These dendriplexes were mixed with bromophenol dye at 1:6 dilution and added to different wells in agarose gel. siPLK1 solution was used as control for comparison. Gel electrophoresis was performed for 35 min at 60 mA in 3% agarose gel containing ethidium bromide. The bands in agarose gel were visualized using UV transilluminator (Gel Doc™ XR+ system, Biorad Laboratories, Inc.) at a wavelength of 365 nm.

2.4 | Particle size and zeta potential

The mean particle size and zeta potential of siPLK1 dendriplexes were measured by zetasizer Nano-ZS (Malvern instrument Ltd., UK) at 25°C. Mean particle size was measured using dynamic light scattering technique. In zeta potential experiment, electrophoretic mobility of the samples was measured in presence of applied electric field.

2.5 | Entrapment efficiency

Quantitative determination of siPLK1 complexed with CPD 3, CPD 4, PAMAM 3, and PAMAM 4 was performed using ribogreen assay. For this purpose, low and high range calibration curve were prepared using reported method (Jones, Yue, Cheung, & Singer, 1998; Sato et al., 2012). To determine entrapment efficiency of siPLK1, dendriplexes of siPLK1 were prepared with CPD 3, CPD 4, PAMAM 3, and PAMAM 4 at N/P ratio 3:1 and centrifuged at 15,000 rpm for 15 min. Supernatants from each sample were collected, diluted with Tris-EDTA buffer and analyzed using microplate reader (Spectramax, Molecular Devices LLC). Entrapment efficiency was calculated using formula given below.

$$\text{Entrapment efficiency}\,(\%) = \frac{\text{Concentration of encapsulated siPLK1}}{\text{Concentration of initial siPLK1}} \times 100.$$

2.6 | Circular dichroism spectrometry

Circular dichroism (CD) spectra of siPLK1 dendriplexes were measured to determine the interaction between siPLK1 and dendrimers (Ferenc et al., 2013; Ionov et al., 2015). Experiment was performed with Jasco, J-815 CD spectrometer (Oklahoma, Japan) between 300 and 200 nm with 0.5 cm path-length using Helma quartz cell. Dendrimer concentration was increased during the experiment and concentration-dependent measurements were made in a 10 mmol/L sodium phosphate buffer, pH 7.4. The recording parameters for CD experiments were as follows: scan speed −50 nm/min, step resolution −1 nm, response time − 2 s, bandwidth −1.0 nm and slit -auto. Spectra are given as the average of at least 3 independent scans. The mean residue ellipticity, Θ (cm^2 $dmol^{-1}$) was calculated using software provided by Jasco. The maximum ellipticity (Θ) values for free siPLK1 and siPLK1 dendriplexes, were calculated and plotted on the graph as a function of dendrimer/siPLK1 charge ratio.

2.7 | Intercalation assay

Fluorescence analysis was performed to study the interaction between siPLK1 and different dendrimers. Samples were prepared by incubation of 0.25 μ*M* fluorescein-labeled siPLK1 with different amounts of dendrimers in 10 mmol/L sodium phosphate buffer (pH 7.4) for 10 min at 25°C. Changes in fluorescence polarization were measured using a Perkin Elmer LS-50B spectrofluorimeter (UK). Polarization was detected at 515 nm (slit 3.5 nm) with excitation at 495 nm (slit 2.5 nm) and expressed as:

$$P = (\mathrm{IV} - G\ \mathrm{IH})/(\mathrm{IV} + G\ \mathrm{IH}).$$

where *G* is a g-factor (calculated automatically by Perkin Elmer software), IV and IH are the vertically and horizontally polarized emission intensities, respectively (de Ruijter et al., 2011).

2.8 | Stability studies

2.8.1 | RNase protection assay

Dendrimer mediated protection of siPLK1 from RNase was determined using RNase protection assay (Ionov et al., 2015). In this experiment, siPLK1 dendriplexes with CPD 3, CPD 4, PAMAM 3, and PAMAM 4 at 3:1 N/P ratio were prepared and treated with RNase (1.25 μg/mL) for 30 min at 37°C. Then samples were kept on ice bath for 5 min followed by addition of heparin solution. Samples were run through agarose gel and migration of siPLK1 was observed using gel electrophoresis (Section 2.3).

2.8.2 | Serum stability assay

Serum stability assay was performed to determine the dendrimer mediated protection of siPLK1 in presence of serum (Koide et al., 2016). For this purpose, siPLK1 dendriplexes with CPD 3, CPD 4, PAMAM 3, and PAMAM 4 at 3:1 N/P ratio were prepared, mixed with equal volume of DMEM supplemented with 10% of FBS and incubated at 37°C. Thirty microliters of sample was collected from stocks of different dendriplex at 0, 0.5, 1, 2, 4, 9, 12, and 24 hr time point and stored in −20°C until gel electrophoresis was performed. Samples were treated with heparin solution and migration of siPLK1 was observed using gel electrophoresis (Section 2.3).

2.9 | In vitro cell culture studies on breast cancer cell lines

2.9.1 | Maintenance of breast cancer cell culture

Breast cancer cell lines (MDA-MB-231 and MCF-7) were procured from the National Center for Cell Science, Pune and cultured in DMEM containing 10% heat inactivated FBS, 1.5 g/L $NaHCO_3$, 2 m*M* L-glutamine, 10,000 units penicillin, 10 μg/mL streptomycin, and 25 μg/mL amphotericin B, incubated at 37°C with 5% CO_2 in a humidified atmosphere.

2.9.2 | Cell uptake study

Cell uptake was performed to study uptake efficiency and internalization of FITC labeled siPLK1 from different dendriplexes using reported method with slight modification (Doppalapudi, Mahira, & Khan, 2017). Both the cell lines were plated separately in 6 well plate (1×10^5 cells/mL) and treated with different formulations (each formulation containing 25 n*M* concentration of siPLK1). The study groups for this experiment were (a) control group (untreated cells), (b) FITC-siPLK1 solution, (c) siPLK1-CPD G3 dendriplex, (d) siPLK1-CPD G4 dendriplex, (e) siPLK1-PAMAM G3 dendriplex, and (f) siPLK1-PAMAM G4 dendriplex. After 2–3 hr, cells were washed with PBS and nuclear staining was performed using acridine orange (AO) stain (1 mg/mL). Images were captured using fluorescent microscope (Nikon Eclipse Microscope, Japan).

2.9.3 | Cell cycle analysis

Cell cycle analysis was performed in MDA-MB-231 and MCF-7 cell lines to examine the mitotic changes and distribution of cells in different phases (sub-G1 vs. G0/G1 vs. S vs. G2/M) (Muntimadugu, Kumar, Saladi, Rafeeqi, & Khan, 2016). Cell lines were plated separately in 6 well plate (1×10^5 cells/well) and treated with different formulations (each formulation containing 250 n*M* conc. of siPLK1) as described in Section 2.7. After 48 hr, cells were trypsinised, washed with PBS, fixed in 70% ethanol and stored overnight at 2–8°C. Then cells were washed, resuspended and treated with RNase A for 15 min to remove the free RNA. The nuclei of cells were stained by propidium iodide reagent (400 μg/mL) and incubated for 30 min at 37°C in dark. The samples were examined using flow cytometer (BD FACSVerse™) and 10,000 events for each sample were analyzed after doublet discrimination module.

3 | RESULTS

3.1 | Formulation development and complexation

Dendriplexes of siPLK1 with CPD 3, CPD 4, PAMAM 3, and PAMAM 4 were prepared and their complexation pattern was studied using agarose gel electrophoresis. Figure 1a1, a2, a3, and a4 represents electropherogram of siPLK1 dendriplexes with CPD 3, CPD 4, PAMAM 3, and PAMAM 4, respectively, at different N/P ratio. In all electropherogram, naked siPLK1 was appeared as a clear band (lane 1). Addition of dendrimer initiated the formation of siPLK1 dendriplex but the band was observed (lane 2, lane 3, and lane 4) due to free siPLK1 until the sufficient quantity of dendrimer was added to occupy all the siPLK1. For siPLK1 dendriplexes with all four dendrimers under study (CPD 3, CPD 4, PAMAM 3, and PAMAM 4), the complexation was observed at 3:1 N/P ratio. Further increase in N/P ratio did not result in appearance of any band in electropherogram.

3.2 | Characterization of dendriplexes and entrapment efficiency

Zeta potential and mean particle size for different dendriplexes of siPLK1 were determined using zetasizer. Change in zeta potential with N/P ratio for dendriplex of siPLK1-CPD 3, siPLK1-CPD 4, siPLK1-PAMAM 3, and siPLK1-PAMAM 4 is indicated in Figure 1b1, b2, b3, and b4, respectively. At complexation point (N/P ratio 3:1), the average zeta potential for siPLK1-CPD 3, siPLK1-CPD 4, siPLK1-PAMAM

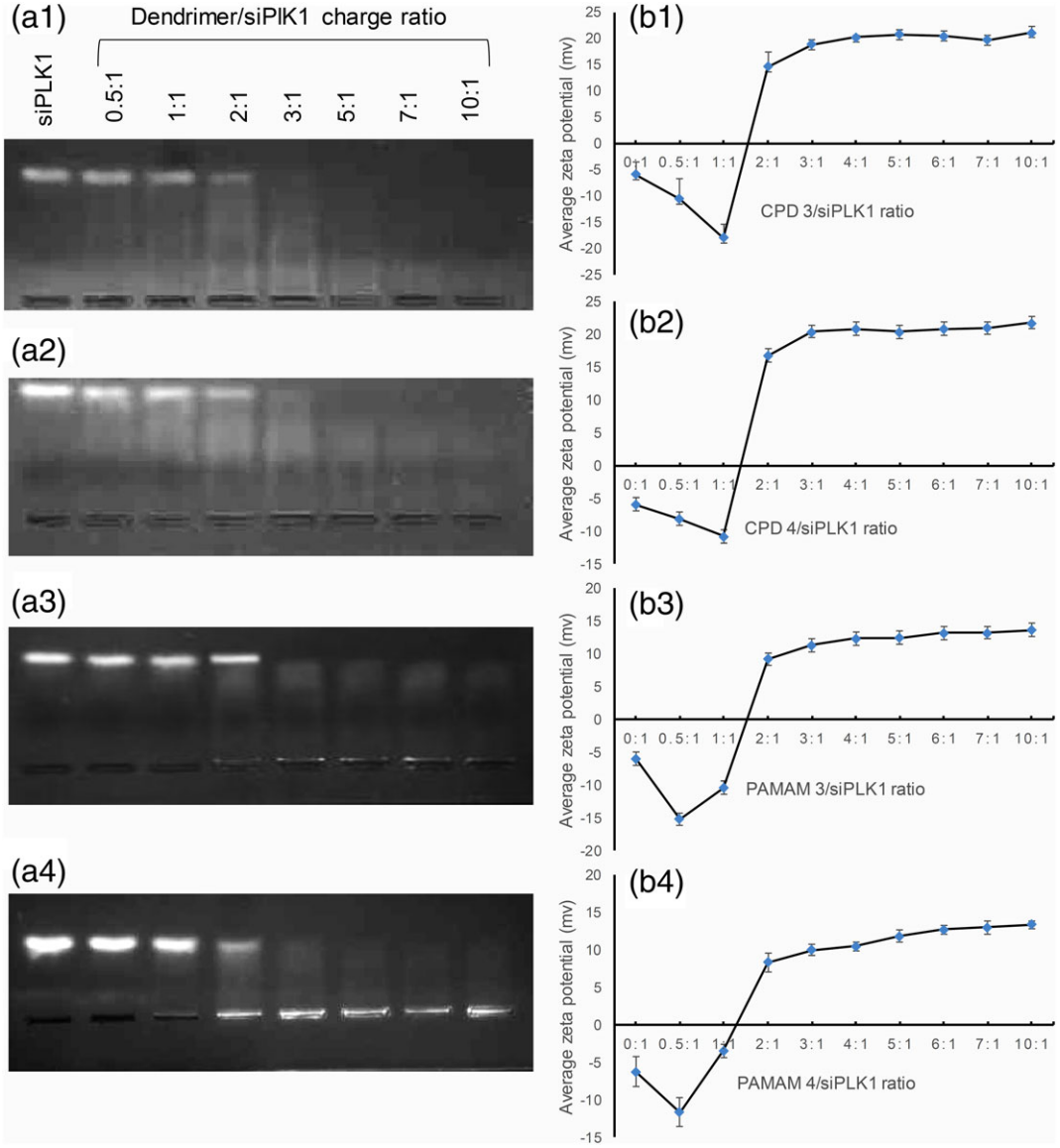

FIGURE 1 Complexation of siPLK1 with dendrimers and zeta potential analysis. Gel electrophoresis was performed to determine complexation of siPLK1 with different dendrimers. (a1) Gel electropherogram of siPLK1-CPD 3 dendriplex, (a2) siPLK1-CPD 4 dendriplex, (a3) siPLK1-PAMAM 3 dendriplex, and (a4) siPLK1-PAMAM 4 dendriplex. Average zeta potential was plotted for different N/P ratio of dendriplexes formed with siPLK1. Change in average zeta potential with increasing N/P ratio of (b1) siPLK1-CPD 3 dendriplex, (b2) siPLK1-CPD 4 dendriplex, (b3) siPLK1-PAMAM 3 dendriplex, and (b4) siPLK1-PAMAM 4 dendriplex. Results represent mean ± *SD* (*n* = 3)

3, and siPLK1-PAMAM 4 were 18.3 ± 0.83, 20.43 ± 1.11, 11.28 ± 0.65, and 9.94 ± 0.76 mV, respectively. Similarly, mean particle size for dendriplexes of CPD and PAMAM dendrimers with siPLK1 were determined. Figure 2a–d indicates mean particle size for different N/P ratio of siPLK1-CPD 3, siPLK1-CPD 4, siPLK1-PAMAM 3, and siPLK1-PAMAM 4 dendriplexes. At 3:1 N/P ratio (complexation point), particle size for dendriplexes of siPLK1-CPD 3, siPLK1-CPD 4, siPLK1-PAMAM 3, and siPLK1-PAMAM 4 were 87.67 ± 9.68, 100.94 ± 12.09, 354.1 ± 20.66, and 140.08 ± 16.1 nm, respectively.

The entrapment efficiency of complexed siPLK1 in different dendriplexes was measured by Quant-iT™ RiboGreen® RNA reagent assay. Entrapment efficiency of siPLK1 with CPD 3, CPD 4, PAMAM 3, and PAMAM 4 was found to be 98.68 ± 1.36%, 96.47 ± 6.43%, 100.30 ± 0.64%, and 97.95 ± 4.03% respectively.

3.3 | Circular dichroism

CD was used to study the effect of dendrimers on secondary structure of siPLK1. The CD spectra for siRNAs are unique with characteristic peaks at 210 and 260 nm (Muntimadugu et al., 2016). Addition of dendrimer induces change in the secondary structure of siRNA. In all dendriplexes of siPLK1 (Figure 3), the ellipticity of complexes decreased with increasing dendrimer/siPLK1 ratio. CD spectra of all dendriplexes also indicated red shift in the characteristic peaks of siRNA (210 and 260 nm) with increasing dendrimer concentration. For dendriplexes of siPLK1-CPD 3 and siPLK1-CPD 4, first characteristic peak was shifted from 210 to 220 nm and second characteristic peak was shifted from 260 to 270 nm. For dendriplexes of siPLK1-PAMAM 3 and siPLK1-PAMAM 4, first peak was shifted from 210 to 230 nm and second characteristic peak was shifted from 260 to 280 nm.

3.4 | Intercalation assay

Fluorescence analysis is widely used technique to study nucleic acid-guest molecule interactions. Figure 4 demonstrates the fluorescence polarization values of FITC labeled siPLK1 and its dendriplexes with dendrimers. Increase in fluorescence polarization values indicated decreased motility of fluorescein molecules attached to siPLK1.

3.5 | Stability studies

3.5.1 | RNase protection assay

RNase protection assay was performed to evaluate the stability of siPLK1 complexed with different dendrimers in presence of RNase enzyme. Figure 5a1, a2, a3, and a4 represented RNase protection assay for siPLK1-CPD 3, siPLK1-CPD 4, siPLK1-PAMAM 3, and siPLK1-PAMAM 4 dendriplexes. First lane of gel electropherogram indicated

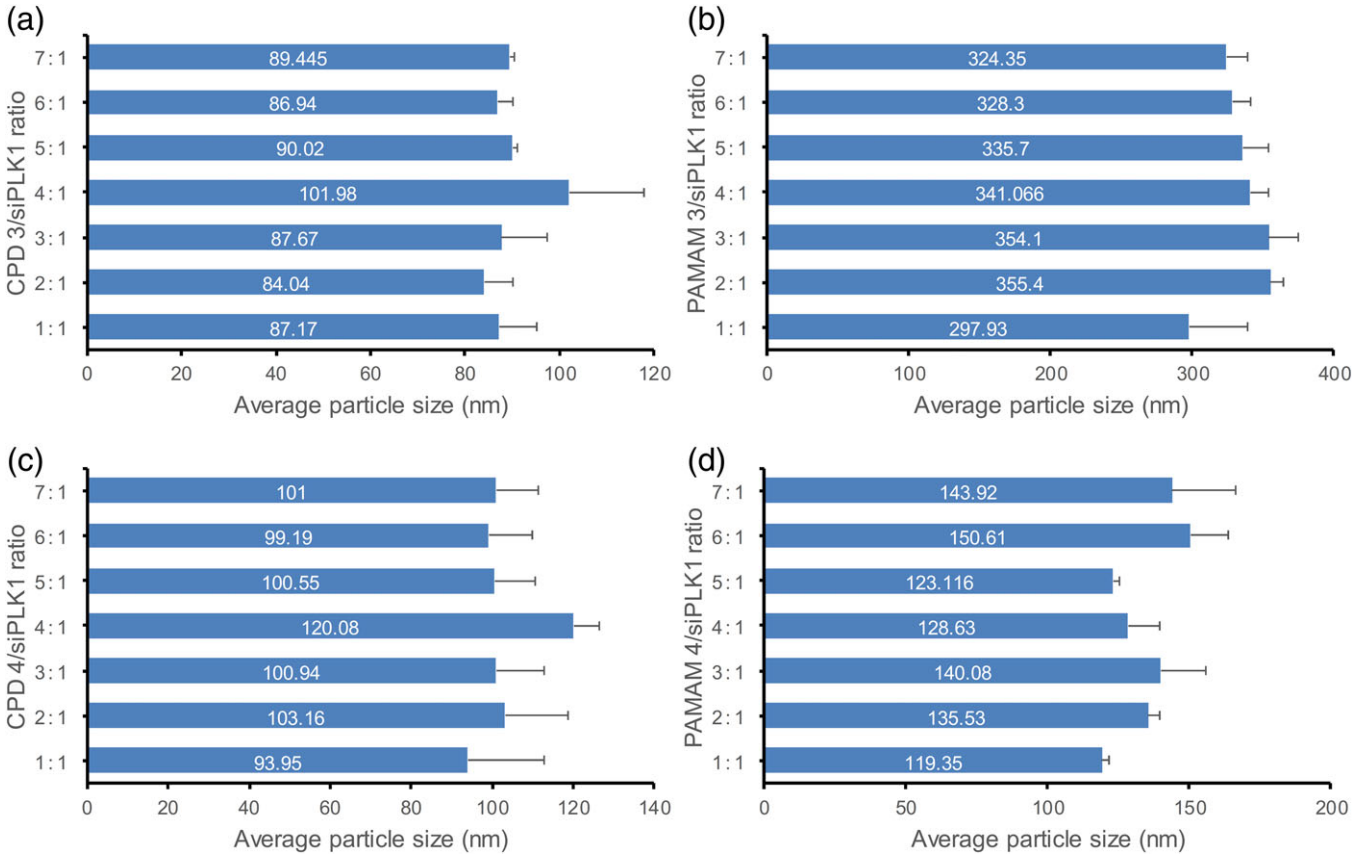

FIGURE 2 Particle size analysis for different dendriplexes of siPLK1. Mean particle size of siPLK1 dendriplexes at different N/P ratio was determined using zetasizer by dynamic light scattering method. Mean particle size of (a) siPLK1-CPD 3 dendriplex, (b) siPLK1-CPD 4 dendriplex, (c) siPLK1-PAMAM 3 dendriplex, and (d) siPLK1-PAMAM 4 dendriplex. Results represent mean ± *SD* (*n* = 3)

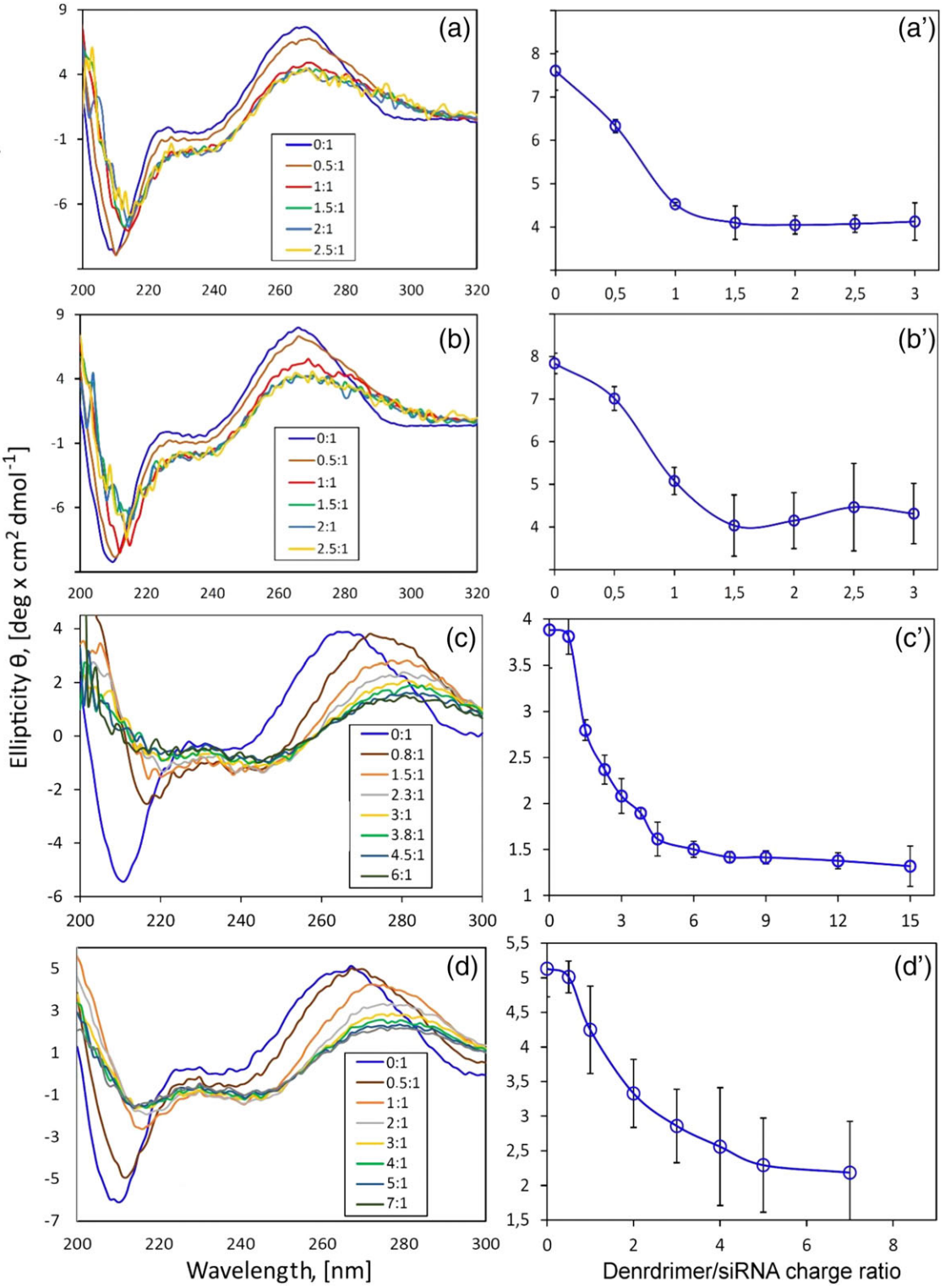

FIGURE 3 CD spectra of dendriplexes of siPLK1. Left panels indicate change in ellipticity of siPLK1 with increase in wavelength at different charge ratio of dendrimer to siPLK1. Right panels indicate the changes in mean residue ellipticity of siPLK1, at Θ_{max} with increasing dendrimer to siRNA charge ratio. (a and a′) CD spectra for siPLK1—CPD 3 dendriplex, (b and b′) CD spectra for siPLK1—CPD 4 dendriplex, (c and c′) CD spectra for siPLK1—PAMAM 3 dendriplex, and (d and d′) CD spectra for siPLK1—PAMAM 4 dendriplex. Results represent mean ± *SD* (*n* = 3)

migration of noncomplexed siPLK1. The second lane containing siPLK1 incubated with RNase indicated no band as the siPLK1 was previously incubated with RNase which resulted in degradation of siPLK1. Third lane represented no band as siPLK1 was complexed with dendrimer. Fourth lane contains siPLK1 dendriplex along with heparin and RNase and this lane was observed with band. The dendriplex protected siPLK1 from degradation by RNase, this siPLK1 was released from dendriplex after addition of heparin and migrated in agarose gel resulting in band

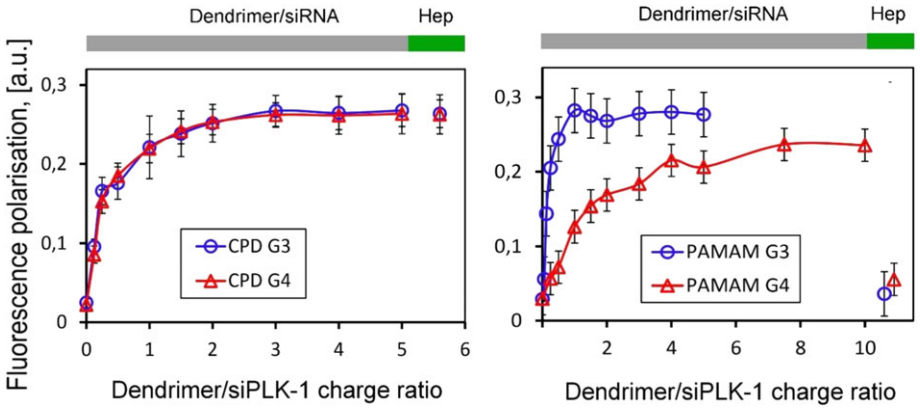

FIGURE 4 Intercalation assay of fluorescent labeled siPLK1 in the presence of different dendrimers. Changes in fluorescence polarization of FITC labeled siPlK1 upon addition of dendrimers at different dendrimer/siRNA charge ratios. Results represent mean ± *SD* (*n* = 3)

appearance. PAMAM 3 and PAMAM 4 dendriplex resulted in more intense band in lane 4 compared to CPD 3 and CPD 4.

3.5.2 | Serum stability assay

Serum stability assay was performed to analyze the stability of siPLK1 dendriplex in presence of serum proteins. Figure 5b1, b2, b3, b4, and b5 showed serum stability assay for siPLK1-CPD 3, siPLK1-CPD 4, siPLK1-PAMAM 3, and siPLK1-PAMAM 4 dendriplexes, respectively. siPLK1 solution was found to be stable till 1 hr indicated by appearance of band in gel electropherogram. No band was observed after 1 hr indicating degradation of siPLK1 in solution. In case of siPLK1 dendriplexes, clear bands were observed until 24 hr.

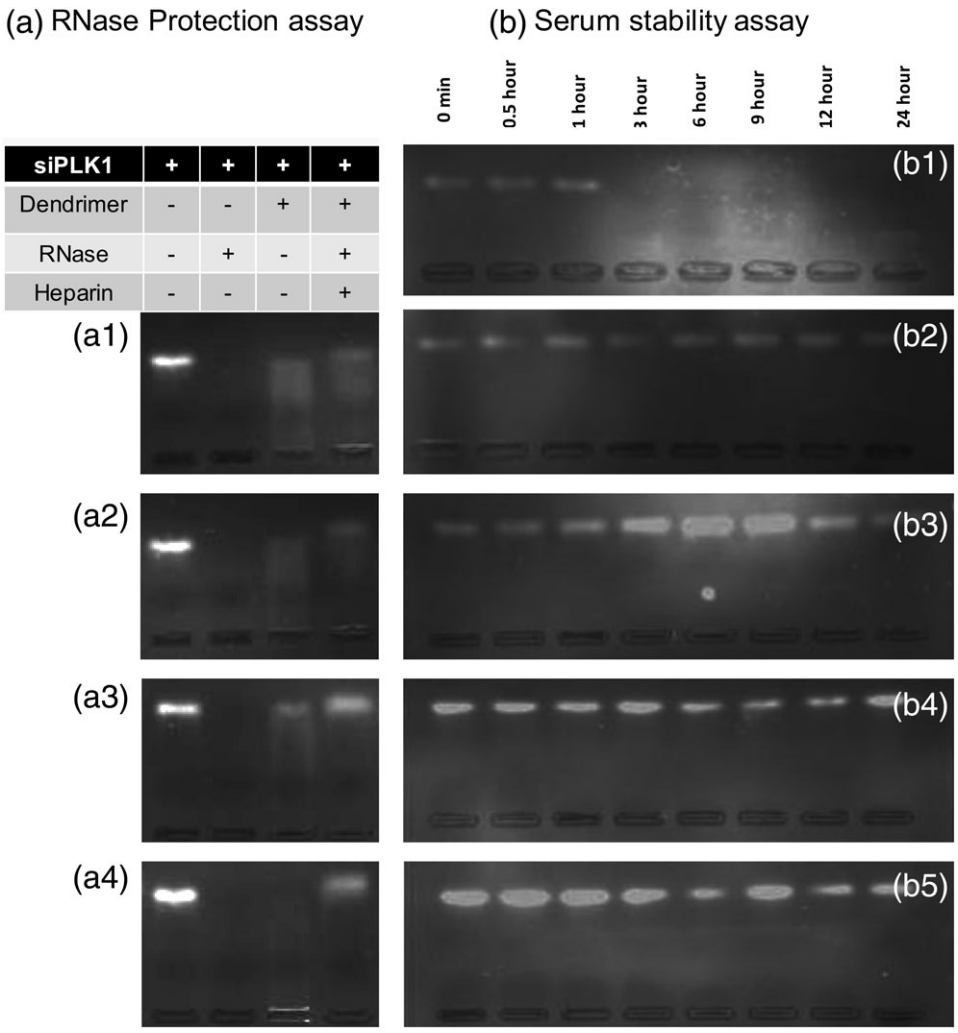

FIGURE 5 Stability studies of siPLK1 dendriplexes in the presence of RNase and serum. (a) RNase protection assay (a1) siPLK1-CPD 3 dendriplex, (a2) siPLK1-CPD 4 lipoplex, (a3) siPLK1-PAMAM 3 dendriplex, and (a4) siPLK1-PAMAM 4 dendriplex. First lane contained noncomplexed siPLK1 resulting migration band. The second lane contained siPLK1 incubated with RNase. Third lane contained dendriplexes of siPLK1 with respective dendrimer. The fourth lane contained siPLK1 dendriplex, RNase and heparin resulting migration band. (b) Serum stability study for (b1) Plain siPLK1 solution, (b2) siPLK1-CPD 3 dendriplex, (b3) siPLK1-CPD 4 lipoplex, (b4) siPLK1-PAMAM 3 dendriplex, and (b5) siPLK1-PAMAM 4 dendriplex

3.6 | In vitro cell culture studies on breast cancer cell lines

3.6.1 | Cell uptake study

Cell uptake was performed in MCF-7 and MDA-MB-231 cells to study the uptake efficiency and internalization of FITC labeled siPLK1 from different dendriplexes (Figure 6). Efficient cell uptake is considered as one of the critical early step to ensure successful delivery. FITC is the widely used fluorophore marker with negligible cell permeation in cell biological interactions. Cells were treated with different FITC-siPLK1 formulations followed by AO staining. FITC produces fluorescence within cytoplasmic region while AO gives green fluorescence in nuclear region. In control groups (Figure 6a,a′), no fluorescence was observed in both the cell lines. siPLK1 solution (Figure 6b,b′) resulted in negligible fluorescence in both the cell lines, that may be due to poor penetration of FITC-siPLK1. In MCF-7 cells dendriplexes formed with CPD (Figure 6c,d) and PAMAM dendrimers (Figure 6e,f) resulted in higher fluorescence intensity in comparison to solution. This is may be due to positive surface charges of dendrimer that favor interactions with cell membrane and the internalization process (Ionov et al., 2012). Generation dependent effect was observed in cell uptake of different dendriplexes where the siPLK1 dendriplexes with CPD 3 (Figure 6c) and PAMAM 3 (Figure 6e) dendrimer resulted in less fluorescent intensity compared to CPD 4 (Figure 6d) and PAMAM 4 (Figure 6f) dendriplexes. Similar results were obtained with MDA-MB-231 cell lines (Figure 6a′–f′).

3.6.2 | Cell cycle analysis

Cell cycle analysis was performed to determine the effect of siPLK1 formulations in specific cell cycle phase arrest of MCF-7 and MDA-MB-231 cell lines. Percentage of cells accumulated in different cell cycle phases and flow cytograms are given in Figure 7. In MCF-7 cell lines (Figure 7a–g), in comparison to control group the percentage of cells at sub-G1 phase was increased from 0.82 to 8.85% with siPLK1 solution, 0.82 to 63.6% with siPLK1-CPD 3 dendriplex, 0.82 to 56.8% with siPLK1-CPD 4 dendriplex, 0.82 to 73.2% with siPLK1-PAMAM 3 dendriplex, and 0.82 to 73% with siPLK1-PAMAM 4 dendriplex.

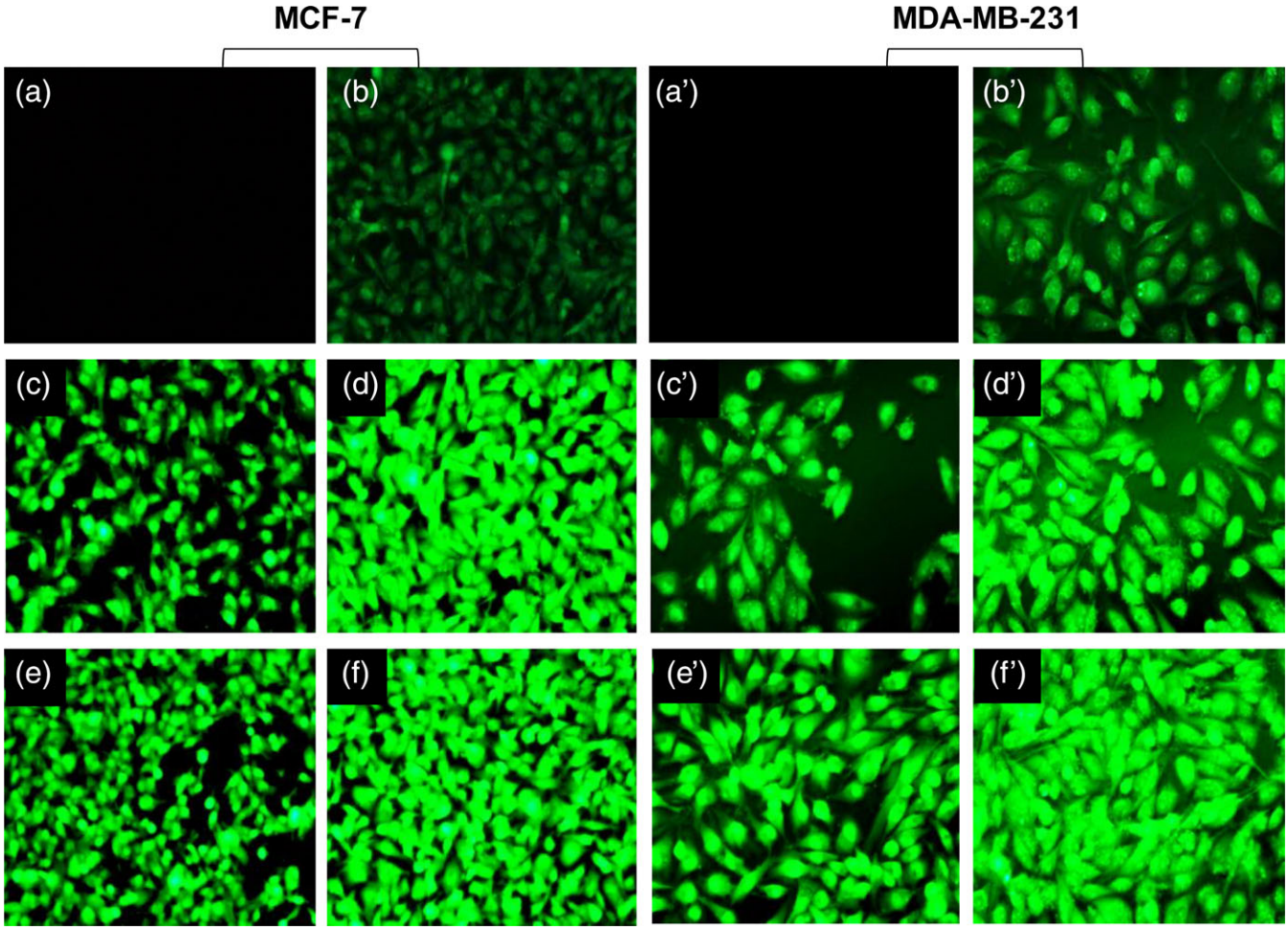

FIGURE 6 Cell uptake analysis for siPLK1 and different dendriplexes. Cell uptake study was performed in MCF-7 and MDA-MB-231 cell lines. FITC labeled siPLK1 was used to determine the internalization of siPLK1 from different formulations. Uptake study in MCF-7 cell lines (a) control, (b) siPLK1 solution, (c) siPLK1-CPD 3 dendriplex, (d) siPLK1-CPD 4 lipoplex, (e) siPLK1-PAMAM 3 dendriplex, and (f) siPLK1-PAMAM 4 dendriplex. Uptake study in MDA-MB-231 cell lines (a′) control, (b′) siPLK1 solution, (c′) siPLK1-CPD 3 dendriplex, (d′) siPLK1-CPD 4 lipoplex, (e′) siPLK1-PAMAM 3 dendriplex, and (f′) siPLK1-PAMAM 4 dendriplex (×200 magnification)

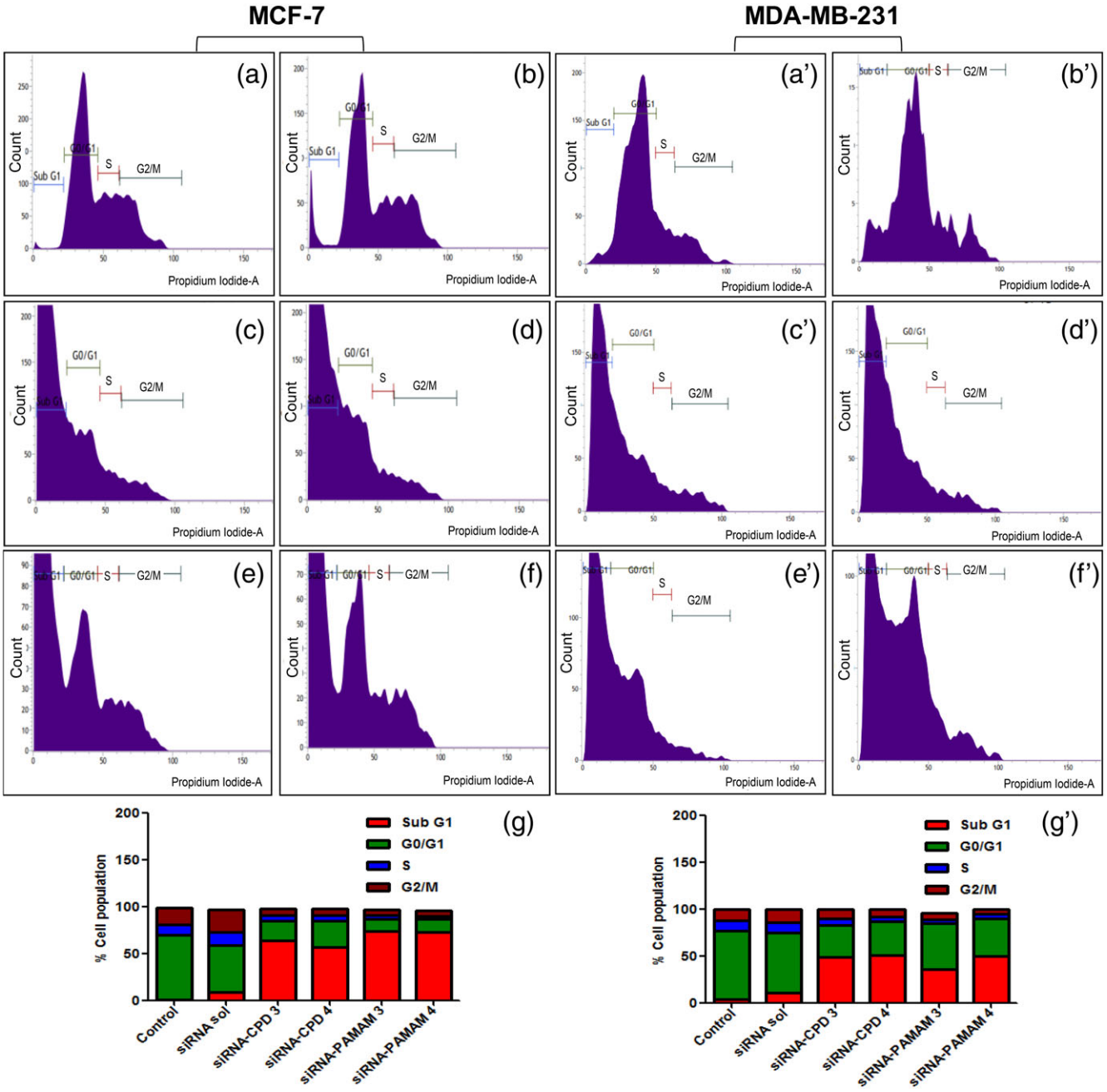

FIGURE 7 Cell cycle analysis using flow cytometry. Cell cycle analysis was performed in MCF-7 and MDA-MB-231 cell lines. In MCF-7 cell lines (a) control, (b) siPLK1 solution, (c) siPLK1-CPD 3 dendriplex, (d) siPLK1-CPD 4 dendriplex, (e) siPLK1-PAMAM 3 dendriplex, (f) siPLK1-PAMAM 4 dendriplex. In MDA-MB-231 cell lines (a′) control, (b′) siPLK1 solution, (c′) siPLK1-CPD 3 dendriplex, (d′) siPLK1-CPD 4 dendriplex, (e′) siPLK1-PAMAM 3 dendriplex, (f′) siPLK1-PAMAM 4 dendriplex, (g) and (g′) graph representing % cell population in cell cycle phases of both the cell lines for different study groups

Similarly, in MDA-MB-231 cell lines (Figure 7a′–g′), compared to control the percentage of cells at sub-G1 phase were increased from 3.51 to 10.4% with siPLK1 solution, 3.51 to 48.5% with siPLK1-CPD 3 dendriplex, 3.51 to 50.6% with siPLK1-CPD 4 dendriplex, 3.51 to 35.7% with siPLK1-PAMAM 3 dendriplex, and 3.51 to 49.7% with siPLK1-PAMAM 4 dendriplex. By this it can be inferred that the induction of apoptosis (sub-G1 peak) is more pronounced with siPLK1 dendriplexes than siPLK1 solution in both the cell lines. Liu et al., also reported that about 90% of PLK1-depleted cells showed sub-G1 DNA at 6 day post transfection suggesting that Plk1-depleted cells undergone apoptosis (Liu & Erikson, 2003).

4 | DISCUSSION

TNBC is the most threatening subtype of breast cancer due to high rate of local and systemic relapse. Standard treatment options are not

defined due to lack of specific receptor subtype on tumor surface. Targeting of such tumors is possible at genomic level and evolution of siRNA therapeutics provided a direction for their targeting. siRNA against PLK1 was reported to be a potential target for TNBC. However, delivery of siRNA is challenging due to its molecular properties and stability concerns. Dendrimers are considered as efficient carriers for siRNA due to their cationic nature and well-defined surface characteristics. Dendriplexes of siPLK1 with phosphorus dendrimers (CPD 3 and CPD 4) and amine dendrimer (PAMAM 3 and PAMAM 4) were prepared and characterized using different techniques (summary of experimental results is displayed in Table 1). Dendriplex formation was determined using gel electrophoresis where the charged molecules moved toward oppositely changed electrode through agarose gel. Even though, initial addition of dendrimer to siPLK1 initiated the formation of siPLK1-dendriplex but the uncomplexed siPLK1 resulted in band formation until the sufficient quantity of dendrimer was added to occupy all the siPLK1. Complexation occurred at N/P ratio 3:1 for all the dendriplexes was confirmed by zeta potential measurement. siPLK1 possess negative zeta potential (−5.99 ± 2.44 mV) and addition of dendrimer resulted in zeta potential shift from negative to positive, near to complexation point (N/P ratio 1:1 to 2:1) for different dendriplexes. After reaching the complexation point (N/P ratio 3:1), zeta potential was almost stabilized and further increase in N/P ratio did not result in major change in zeta potential. Zeta potential data show, that dendriplexes formed with CPD dendrimers charged more positively than PAMAM ones. This fact leads to conclusion that complexes formed with CPD dendrimers can be uptaken by cells more effectively. CD spectra and intercalation assay further supported the conclusion that both dendrimers electrostatically attracted and binds siPLK1 near to N/P ratio 2:1 to 3:1, on the other hand, PAMAM dendrimer affect the secondary structure of siRNA stronger whose spectra shape significantly changed. The presence of CPD dendrimers caused only small changes in the general shape of the siPLK1 spectra with weaker exhibition of red shift effect. Particle size for dendriplexes did not show much difference with increasing N/P ratio. The entrapment of siPLK1 with all the dendrimers was nearly 100% and dendriplexes were found to be stable in presence of serum for 24 hr. Dendriplexes protected the siPLK1 from RNase induced degradation. siPLK1 incubated with RNase showed no band whereas siPLK1 dendriplexes incubated with RNase indicated band after heparin treatment (heparin released siPLK1 from dendriplex). PAMAM 3 and PAMAM 4 dendriplex resulted in more intense band compared to CPD 3 and CPD 4. This could be due to stronger binding ability of CPD dendrimers toward siPLK1 in comparison to PAMAM dendrimer. Hence, it is likely that the same concentration of heparin is ineffective in displacing siRNA from the complex.

Cell culture experiments were performed using MDA-MB-231 and MCF-7 cell lines. MDA-MB-231 is highly aggressive, invasive, and poorly differentiated cell line lacking ER, PR expression, as well as HER2 amplification. The invasiveness of the MDA-MB-231 cells is mediated by proteolytic degradation of the extracellular matrix which is similar to invasive cancer cells thus, MDA-MB-231 cell line is considered as model for study of TNBC (Chavez et al., 2010; Liu, Zang, Fenner, Possinger, & Elstner, 2003). Cell uptake in MDA-MB-231 and MCF-7 cell lines indicated more intracellular distribution of FITC conjugated siPLK1 from dendriplexes compared to siPLK1 solution. This could be due to dendrimer mediated enhanced penetration of siPLK1 into the cells. These dendriplexes also showed generation dependent internalization, where the CPD 4 and PAMAM 4 resulted in more accumulation of FITC-siPLK1 compared to CPD 3 and PAMAM

TABLE 1 Summary of results for experiments performed to determine complexation, stability, and in vitro activity of siPLK1 dendriplexes

S. No.	Experiments		CPD 3 dendriplex	CPD 4 dendriplex	PAMAM 3 dendriplex	PAMAM 4 dendriplex
1.	Complexation (N/P ratio)		3:1	3:1	3:1	3:1
2.	Particle size in nm (at 3:1 N/P ratio)		87.67 ± 9.68	100.94 ± 12.09	354.1 ± 20.66	140.08 ± 16.1
3.	Zeta potential in mV (at 3:1 N/P ratio)		18.3 ± 0.83	20.43 ± 1.11	11.28 ± 0.65	9.94 ± 0.76
4.	Entrapment efficiency (%)		98.68 ± 1.36	96.47 ± 6.43	100.30 ± 0.64	97.95 ± 4.03
5.	Circular dichroism	Reduction in ellipticity with increasing concentration of siPLK1	+ +	+ +	+ + +	+ + +
		Red shift at wavelength (210 and 260 nm)	+ +	+ +	+ + +	+ + +
6.	Stability in the presence of RNase		Stable	Stable	Stable	Stable
7.	Stability in serum		Stable	Stable	Stable	Stable
8.	Cell uptake in MCF-7 cell line (comparison to siPLK1 solution)		+ +	+ + +	+ +	+ + +
9.	Cell uptake in MDA-MB-231 cell line (comparison to siPLK1 solution)		+ +	+ + +	+ +	+ + +
10.	Cell cycle analysis in MCF-7 cell line (cell population in sub-G1 phase in comparison to control)		0.82–63.6%	0.82–56.8%	0.82–73.2%	0.82–73%
11.	Cell cycle analysis in MDA-MB-231 cell line (cell population in sub-G1 phase in comparison to control)		3.51–48.5%	3.51–50.6%	3.51–35.7%	3.51–49.7%

Note. Indication for the symbols used in this table: + + + marked, + + moderate, + slight.

3. Surface charge density increases with increasing the generation of dendrimer providing more surface groups for interaction with siRNA. Hence, higher generation 4 dendrimer provided more cellular uptake than generation 3 dendrimers.

siPLK1 is reported to arrest the cells in sub-G1 phase (Yunoki, Tabuchi, Hayashi, & Kondo, 2013), however, inability of naked siPLK1 to efficiently penetrate the cell and their susceptibility toward RNase and serum mediated degradation reduce the efficiency of naked siPLK1. Cell cycle analysis indicated increased cell population in sub-G1 phase (marker of apoptosis) in dendriplexes treated groups compared to siPLK1 solution. However, significant difference was not observed in % cell arrest (sub-G1 phase) between the dendriplexes formed with PAMAM and CPD dendrimers. This indicated that the structural difference in PAMAM and CPD dendrimer did not affect the cell arrest induced by siPLK1. Both the classes of dendrimers protected the siPLK1 in different biological conditions and facilitated efficient penetration, thereby improving the efficacy of siPLK1 to induce apoptosis. Results indicated the suitability of both PAMAM and CPD dendrimers for the delivery of siPLK1 in the treatment of TNBC.

ACKNOWLEDGMENTS

Authors are thankful to Director NIPER-Hyderabad for providing required facilities, support, and encouragement throughout the project. Authors also thank Mr. Nagavendra Kommineni for his valuable suggestions and inputs in preparation of manuscript.

CONFLICT OF INTEREST

The authors report no financial interest that might pose a potential, perceived, or real conflict.

ORCID

Maksim Ionov https://orcid.org/0000-0001-7227-6864

REFERENCES

Brenton, J. D., Carey, L. A., Ahmed, A. A., & Caldas, C. (2005). Molecular classification and molecular forecasting of breast cancer: Ready for clinical application? *Journal of Clinical Oncology*, *23*(29), 7350–7360.

Chavez, K. J., Garimella, S. V., & Lipkowitz, S. (2010). Triple negative breast cancer cell lines: One tool in the search for better treatment of triple negative breast cancer. *Breast Disease*, *32*(1–2), 35–48.

de Ruijter, T. C., Veeck, J., de Hoon, J. P., van Engeland, M., & Tjan-Heijnen, V. C. (2011). Characteristics of triple-negative breast cancer. *Journal of Cancer Research and Clinical Oncology*, *137*(2), 183–192.

Dent, R., Trudeau, M., Pritchard, K. I., Hanna, W. M., Kahn, H. K., Sawka, C. A., … Narod, S. A. (2007). Triple-negative breast cancer: Clinical features and patterns of recurrence. *Clinical Cancer Research*, *13*(15), 4429–4434.

Doppalapudi, S., Mahira, S., & Khan, W. (2017). Development and in vitro assessment of psoralen and resveratrol co-loaded ultradeformable liposomes for the treatment of vitiligo. *Journal of Photochemistry and Photobiology, B: Biology*, *174*, 44–57.

Du, J., Sun, Y., Shi, Q.-S., Liu, P.-F., Zhu, M.-J., Wang, C.-H., … Duan, Y.-R. (2012). Biodegradable nanoparticles of mPEG-PLGA-PLL triblock copolymers as novel non-viral vectors for improving siRNA delivery and gene silencing. *International Journal of Molecular Sciences*, *13*(1), 516–533.

Dzmitruk, V., Szulc, A., Shcharbin, D., Janaszewska, A., Shcharbina, N., Lazniewska, J., … Klajnert-Maculewicz, B. (2015). Anticancer siRNA cocktails as a novel tool to treat cancer cells. Part (B). Efficiency of pharmacological action. *International Journal of Pharmaceutics*, *485*(1), 288–294.

Ferenc, M., Pedziwiatr-Werbicka, E., Nowak, K. E., Klajnert, B., Majoral, J.-P., & Bryszewska, M. (2013). Phosphorus dendrimers as carriers of siRNA-characterisation of dendriplexes. *Molecules*, *18*(4), 4451–4466.

Hu, K., Law, J. H., Fotovati, A., & Dunn, S. E. (2012). Small interfering RNA library screen identified polo-like kinase-1 (PLK1) as a potential therapeutic target for breast cancer that uniquely eliminates tumor-initiating cells. *Breast Cancer Research*, *14*(1), 22–30.

Ionov, M., Lazniewska, J., Dzmitruk, V., Halets, I., Loznikova, S., Novopashina, D., … Milowska, K. (2015). Anticancer siRNA cocktails as a novel tool to treat cancer cells. Part (A). Mechanisms of interaction. *International Journal of Pharmaceutics*, *485*(1), 261–269.

Ionov, M., Wróbel, D., Gardikis, K., Hatziantoniou, S., Demetzos, C., Majoral, J. P., … Bryszewska, M. (2012). Effect of phosphorus dendrimers on DMPC lipid membranes. *Chemistry and Physics of Lipids*, *165*, 408–413.

Jain, A., Hosseinkhani, H., Domb, A. J., & Khan, W. (2015). Cationic polymers for the delivery of therapeutic nucleotides. In G. Ramawat, J.-M. Mérillon (Eds.), *Polysaccharides: Bioactivity and biotechnology* (pp. 1969–1990). Springer Nature Switzerland: Springer.

Jones, L. J., Yue, S. T., Cheung, C.-Y., & Singer, V. L. (1998). RNA quantitation by fluorescence-based solution assay: RiboGreen reagent characterization. *Analytical Biochemistry*, *265*(2), 368–374.

Koide, H., Okamoto, A., Tsuchida, H., Ando, H., Ariizumi, S., Kiyokawa, C., … Oku, N. (2016). One-step encapsulation of siRNA between lipid-layers of multi-layer polycation liposomes by lipoplex freeze-thawing. *Journal of Controlled Release*, *228*, 1–8.

Liu, H., Zang, C., Fenner, M., Possinger, K., & Elstner, E. (2003). PPARγ ligands and ATRA inhibit the invasion of human breast cancer cells in vitro. *Breast Cancer Research and Treatment*, *79*(1), 63–74.

Liu, X., & Erikson, R. L. (2003). Polo-like kinase (Plk) 1 depletion induces apoptosis in cancer cells. *Proceedings of the National Academy of Sciences*, *100*(10), 5789–5794.

Mdzinarashvili, T., Khvedelidze, M., Shekiladze, E., Shengelia, N., & Hianik, T. (2018). Thermodynamic properties of DNA-dendrimer complexes and features of their applications. *General Physiology and Biophysics*, *37*(5), 597–601.

Muntimadugu, E., Kumar, R., Saladi, S., Rafeeqi, T. A., & Khan, W. (2016). CD44 targeted chemotherapy for co-eradication of breast cancer stem cells and cancer cells using polymeric nanoparticles of salinomycin and paclitaxel. *Colloids and Surfaces, B: Biointerfaces*, *143*, 532–546.

Pandi, P., Jain, A., Kommineni, N., Ionov, M., Bryszewska, M., & Khan, W. (2018). Dendrimer as a new potential carrier for topical delivery of siRNA: A comparative study of dendriplex vs. lipoplex for delivery of TNF-α siRNA. *International Journal of Pharmaceutics*, *550*(1–2), 240–250.

Pandi, P., Jain, A., Raju, S., & Khan, W. (2017). Therapeutic approaches for the delivery of TNF-α siRNA. *Therapeutic Delivery*, *8*(5), 343–355.

Pecot, C. V., Calin, G. A., Coleman, R. L., Lopez-Berestein, G., & Sood, A. K. (2010). RNA interference in the clinic: Challenges and future directions. *Nature Reviews. Cancer*, *11*(1), 59–67.

Sato, Y., Hatakeyama, H., Sakurai, Y., Hyodo, M., Akita, H., & Harashima, H. (2012). A pH-sensitive cationic lipid facilitates the

delivery of liposomal siRNA and gene silencing activity in vitro and in vivo. *Journal of Controlled Release*, *163*(3), 267–276.

Strebhardt, K., & Ullrich, A. (2006). Targeting polo-like kinase 1 for cancer therapy. *Nature Reviews. Cancer*, *6*(4), 321–330.

Yunoki, T., Tabuchi, Y., Hayashi, A., & Kondo, T. (2013). Inhibition of polo-like kinase 1 promotes hyperthermia sensitivity via inactivation of heat shock transcription factor 1 in human retinoblastoma Cellsplk1 and HT in human retinoblastoma cells. *Investigative Ophthalmology & Visual Science*, *54*(13), 8353–8363.

How to cite this article: Jain A, Mahira S, Majoral J-P, Bryszewska M, Khan W, Ionov M. Dendrimer mediated targeting of siRNA against polo-like kinase for the treatment of triple negative breast cancer. *J Biomed Mater Res*. 2019; 1–12. https://doi.org/10.1002/jbm.a.36701